Optics Letters

Optical-spatial-summing-based NOMA with fine-grained power allocation for VLC-enabled IoT applications

Chao Hu,[1,†] Chen Chen,[2,†] Min Guo,[1] Yanbing Yang,[1,3,*] Jun Luo,[4] and Liangyin Chen[1,3]

[1]College of Computer Science, Sichuan University, Chengdu 610065, China
[2]School of Microelectronics and Communication Engineering, Chongqing University, Chongqing 400044, China
[3]Institute for Industrial Internet Research, Sichuan University, Chengdu 610065, China
[4]School of Computer Science and Engineering, Nanyang Technological University, Singapore 639798, Singapore
*Corresponding author: yangyanbing@scu.edu.cn

Received 27 July 2020; accepted 2 August 2020; posted 5 August 2020 (Doc. ID 403914); published 31 August 2020

In this Letter, we propose and demonstrate a practical optical-spatial-summing-based non-orthogonal multiple access (OSS-NOMA) technique for visible light communication (VLC) systems. This technique is innovative in adopting OSS in that the transmitter of OSS-NOMA VLC can be built upon commercial illuminating light emitting diodes (LEDs), free of LEDs' harmful nonlinearity. Unlike conventional NOMA VLC using analog components such as digital-to-analog converters and bias-T in the transmitter side, OSS-NOMA exploits only digital control signals to drive a LED array in forming optical power superposition for NOMA signals. We demonstrate that by simply switching different amounts of LED chips on or off, the proposed OSS-NOMA transmitter can deliver a fine-grained power allocation ratio ranging from 0.01 to one for two users. The implemented OSS-NOMA VLC prototype leveraging commercial components can achieve low bit error rates of ≤3.1 × 10^{-3} for two users at a data rate of 800 kbps, confirming the promising potential of this novel OSS-NOMA VLC for Internet of Things (IoT) applications.

https://doi.org/10.1364/OL.403914

Given the increasing deployments of light emitting diode (LED) lighting infrastructure, illuminating LEDs enabling visible light communication (VLC) for Internet of things (IoT) applications have attracted extensive attention from many researchers. This is attributed mainly to the inherent merits (e.g., huge license-free spectrum, low-cost components, and high density access) of such VLC settings; they match the requirements of many IoT applications generally more concerned with massive device connections than data rates [1,2]. However, the access capability provided by such VLC systems is seriously limited by the usable bandwidth of commercial-off-the-shelf (COTS) illuminating LEDs [3]. Recently, advanced non-orthogonal multiple access (NOMA) schemes have been considered to be able to alleviate this bandwidth limitation [4–6], because multiplexing in NOMA is performed in the electrical and/or optical power domain rather than in the conventional frequency. Many pioneering works have already verified the promising performance on capacity enhancement of electrical power domain NOMA VLC [5,7–9]. For example, [5] proposes a flexible-rate successive interference cancellation (SIC)-free NOMA scheme to improve data rates by extending the effective power allocation ratio (PAR) range, and [7] proposes a power allocation strategy by considering user fairness.

Although using NOMA techniques in VLC can exactly improve the system capacity, most existing works ignore the key issue of LEDs' nonlinearity, which significantly degrades the expected gains offered by advanced NOMA technology. In order to suppress LED nonlinearity while maintaining relatively low system complexity, a new technique inspired by the beamforming technology in radio communication, namely, optical spatial summing (OSS) modulation, has been proposed, and its superiority to traditional single-carrier- or orthogonal frequency division multiplexing (OFDM)-based VLC systems has also been verified [3,10–12]. Inspired by this idea, a recent work in [4] has implemented a hybrid NOMA scheme by integrating OSS modulation into traditional NOMA VLC to partially retain LEDs' nonlinear distortion. However, it has to use two conventional analog chains, such as a digital-to-analog converter (DAC) and bias-T, to reduce the maximum driving current so as to fit the LEDs' narrow dynamic range. On the contrary, the OSS modulation is able to modulate data onto light intensity via a fully digital chain, i.e., only on–off logic, without any analog control signals, so as to address LED nonlinearity yet maintain low complexity.

To this end, we propose and demonstrate a low-complexity and cost-efficient OSS-NOMA VLC system in this Letter. To address the nonlinearity issue of illuminating LED chips, we design a novel transmitter driven only by digital signals so as to remove the traditional analog components such as DAC and bias-T on the transmitter side. By simply switching on or off the LED chips, the realized transmitter of our proposed OSS-NOMA VLC system can deliver a fine-grained optical output

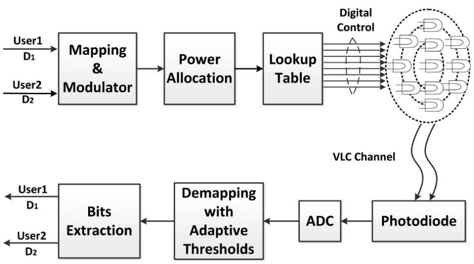

Fig. 1. Block diagram of the proposed OSS-NOMA VLC system for two users.

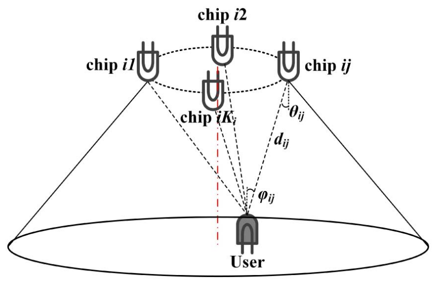

Fig. 2. Modeling the OSS modulation from the i-th group containing K_i LED chips.

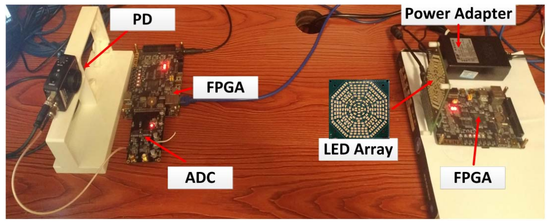

Fig. 3. Prototype of the novel OSS-NOMA VLC system.

with a PAR ranging from 0.01 to one, whereas the system in [4] can obtain only four types of PARs in the optical domain. To further reduce the control logic, a look-up table (LUT) scheme is proposed to fast match the expected PARs to the digital control codes. By implementing an OSS-NOMA VLC prototype leveraging field-programmable gate array (FPGA) and illuminating LED chips, we extensively evaluate its performance, and the experiment results show that it can achieve low bit error rates (BERs) of $\leq 3.1 \times 10^{-3}$ for two users at a data rate of 800 kbps, satisfying the need of many IoT applications.

The schematic block diagram for the proposed OSS-NOMA VLC with two users is illustrated in Fig. 1. The input data of both two users are fed into the mapping and modulator block to generate modulated symbols, where on–off keying (OOK) modulation is used for data mapping in this Letter to quickly verify our novel idea of OSS-NOMA VLC, and the other modulation schemes are also applicable. Subsequently, the modulated symbols are allocated to a predefined power ratio according to the users' channel gains. Finally, we use the allocated power ratio as an index to seek out its corresponding control code from the power ratio LUT, which is created and stored in the transmitter, as described in the following paragraphs, to directly drive the LED array for emitting modulated light. It is the prime difference between our OSS-NOMA VLC and traditional ones such as the latest work of [4], which still used cumbersome DACs and bias-Ts to drive LEDs, as shown in Fig. 3 of [4].

The LED array designed in this Letter has a disk shape as shown in Fig. 1 that consists of 255 phosphor-based white LED chips and low-cost driving transistors of MMSS8050 to mimic a COTS luminaire used in our daily lives. In particular, we arrange those 255 LED chips in a group manner, where we put one LED chip at the center of the array as the first group and the last group containing 128 chips at the periphery, so that only eight digital control signals are enough to handle all 255 LED chips. Figure 2 depicts the principle of OSS modulation of K_i LED chips in one group of the LED array. As all the LED chips have only two states, by using a binary control process $x_{ij}(t) \in \{0, 1\}$ for each chip and assuming that a total of G groups of LEDs are used, the overall spatially superposed light intensity at the photodiode (PD) can hence be obtained by

$$y(t) = \sum_{i=1}^{G} \sum_{j=1}^{K_i} R h_{ij} x_{ij}(t) + n(t), \quad (1)$$

where R is the responsivity of the PD, h_{ij} is the channel gain between the j-th LED chip of the i-th group and the PD [13], and $n(t)$ is the corresponding additive thermal and shot noises. The additive nature of Eq. (1) confirms that the spatial summing effect of multiple on–off control processes should lead to a linear increase in received optical power at the receiver side. Therefore, we can assign different numbers of LED chips to different users based on the configured PAR LUT to deliver the corresponding powers with only digital on–off control.

In order to verify the idea of OSS-NOMA VLC, we implement a COTS device based the proof-of-concept transmitter shown in Fig. 3. The novel transmitter of the OSS-NOMA VLC consists of a LED array and a FPGA board, which can be powered by a commercial 12-V power adaptor with a maximum driving current of 2 A. In particular, the LED array carrying 255 low-cost phosphor-based white LED chips is built on a four-layer printed circuit board (PCB) that is hosted directly by the FPGA main board. Since we creatively separate those 255 LEDs into eight groups with power-of-two arrangement, i.e., each group has 2^i chips and $i = 0, 1, \cdots, 7$, only eight digital control signals are enough to handle all 255 LED chips. The similar work of [4] still needs two DACs and bias-Ts to drive nine LED chips with a very limited dynamic range for usable power ratio, but our transmitter can yield various PARs within the full range from 0.01 to one, as depicted in Fig. 4(a). Here we define the PAR as $\alpha = P_1/P_2$, where P_1 and P_2 are allocated powers for user1 and user2, respectively. To satisfy the lighting requirement of the VLC transmitter used mainly for indoor illumination, the total emission power of the LED array is generally assumed to be a constant C, i.e., $P_1 + P_2 = C$. Although a few tiny fluctuations are observed on the measured power ratio of PAR due to the chip diversity, particular circuit setting, and control codes, which can be calibrated manually via cumbersome hardware troubleshoots, there is a much easier method by simply sorting the measured values and updating the PAR LUT correspondingly. Figure 4(b) clearly shows that the calibrated results are exactly following the ground truth.

We use an AX7020 FPGA to mix the two users' data streams and perform OOK modulation for generating the control signals for the LED array, as illustrated in Fig. 3, at the transmitter side. In this Letter, we consider the sampling rate as a configurable parameter that will be evaluated as the transmission frequency (T_f) in the experiment section. We add a header including 40 symbols of zero power (P_0), user1's power of

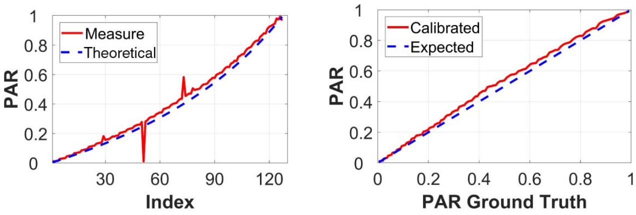

(a) Measured PAR. (b) Calibrated PAR table.

Fig. 4. Adaptive calibration for PAR table.

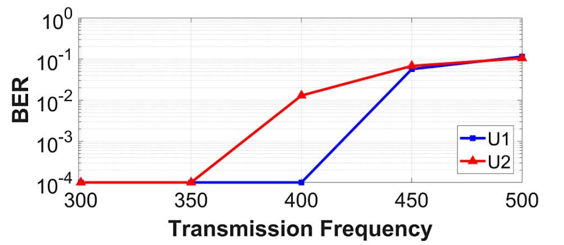

Fig. 6. BER versus transmission frequency (T_f) with PAR = 0.4.

P_1, user2's power of P_2, and maximum optical power of the transmitter ($P_{\max}$) into each session (total 2000 symbols for two users), as illustrated in Figs. 5(a) and 5(c), for indicating the start of a transmission session and assisting demodulating threshold configuration.

At the receiver side, as shown in Fig. 3, we use a PD of PDA36A without a lens as the receiver front-end to capture the superposed modulated light and convert it to electrical signal. A 12-bit analog-to-digital converter (ADC) daughter board consisting of AD9226 is used to sample the received electrical signal and pass a discretely digital data stream to the FPGA main board. The FPGA can perform the whole demodulation procedure locally or forward the data to a computer with MATLAB via Ethernet. In general, we first locate the predefined headers in the received data stream (RDS), and then set the corresponding thresholds, i.e., TH_{11}, TH_{12}, and TH_{13}, as shown in Figs. 5(a) and 5(c), for demapping and demodulation based on the allocated power for each user. Taking advantage of delicate header design in the transmission session as aforementioned, we actually have obtained the corresponding received signal strength for the assigned power of each user, which can be used to estimate the demodulating thresholds, after locating the header. In general, the nth user can receive four types of signal strength [defined as Vnr_i in Eq. (2)] according to our header generation scheme in a typical NOMA VLC system for two users. Therefore, the thresholds can be further estimated as

$$\mathrm{TH_{ni}} = \frac{V_{nr(i+1)} + V_{nr_i}}{2}, \quad \begin{cases} n = 1, 2 \\ i = 1, 2, 3 \end{cases}. \tag{2}$$

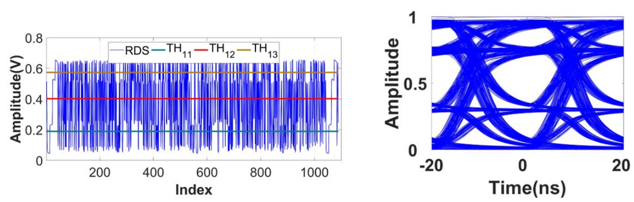

(a) Waveform with PAR=0.4 (b) Eye diagram with PAR=0.4

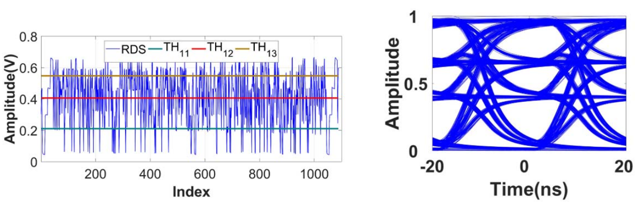

(c) Waveform with PAR=0.6 (d) Eye diagram with PAR=0.6

Fig. 5. Illustration of the received waveforms with demodulating thresholds and corresponding eye diagrams.

Intuitively, we can obtain the three thresholds for demodulating four types of reception signal strength in our current implementation with two users. In particular, for the relatively high power of user2, only one threshold of TH_{22} is required. With this simple method, it is able to demodulate users' data without SIC, which is generally applied in conventional NOMA VLC.

Since the superiority of OSS modulation compared to conventional ones has been verified directly in [3], we do not report the comparison results in this paper but focus on evaluating the transmission performance of the proposed OSS-NOMA VLC transmitter. We change the transmission frequency (T_f) from 300 to 500 kHz, and position the near user (user1) and far user (user2) at distances of 40 and 100 cm from the transmitter, respectively. As for the PAR configuration, we intuitively set it as 0.4 to simply follow the ratio of two users' distance: $\frac{40}{100}$. The results for two users are illustrated in Fig. 6, and here we set a BER error floor of 10^{-4} to regulate the BER plot. As we would expect, the near user1 can support a relatively higher transmission frequency of 400 kHz with a low BER of 10^{-4}, while user2 has a BER of around 0.013 in the same condition due to the signal attenuation.

Figure 7(a) illustrates the BER performance of the proposed OSS-NOMA VLC under a changing PAR at two transmission frequencies. Similar to the above evaluation, user1 has better overall performance in terms of BER than user2 due to a shorter transmission distance resulting in a good signal-to-noise ratio (SNR). In particular, user1 can support a wider PAR dynamic range with the floor BER of $\leq 10^{-4}$ from 0.3 to 0.7 for 400 kHz, while user2's range is nearly half that of user1's, say from 0.01 to 0.2 at a transmission frequency of 400 kHz. However, the available PAR range can be wider if the transmission frequency is reduced to 300 kHz, as shown in Fig. 7(a). For the case of high PARs over 0.7, the BERs increase rapidly with the increase in PAR for both users. The corresponding eye diagrams are shown in Figs. 7(b)–7(g). Nonetheless, the experimental results strongly confirm the feasibility of the proposed OSS-NOMA VLC system for multiple users, delivering reasonable data rates under appropriate system configuration.

We now evaluate the average BER of the proposed OSS-NOMA scheme for user1 and user2. As in the previous experiment settings, we position user1 and user2 at distances of 40 and 100 cm from the transmitter, respectively, vary the transmission frequency (T_f) from 300 to 500 kHz, and change the PAR from 0.01 to 0.99. As observed above, running at a lower transmission frequency can always obtain good BERs for both users so that the average BER is also low, as reported in Fig. 8. Specifically, user2 cannot obtain a satisfying BER when running at 400 kHz with any PAR in Fig. 7(a), but the average BER achieves a tradeoff, dropping to 3.1×10^{-3} when PAR is

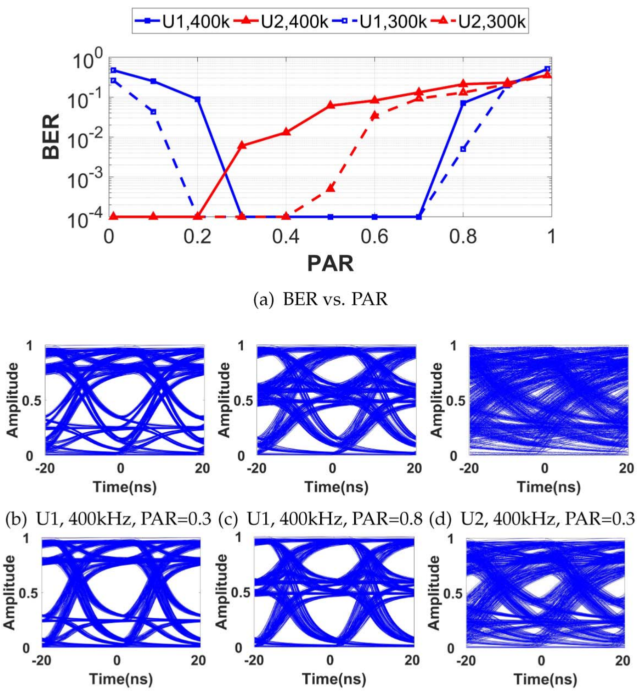

(a) BER vs. PAR

(b) U1, 400kHz, PAR=0.3 (c) U1, 400kHz, PAR=0.8 (d) U2, 400kHz, PAR=0.3

(e) U1, 300kHz, PAR=0.3 (f) U1, 300kHz, PAR=0.8 (g) U2, 300kHz, PAR=0.3

Fig. 7. BER versus PAR with corresponding eye diagrams at transmission frequencies of 400 kHz and 300 kHz.

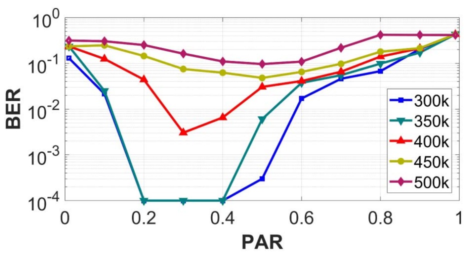

Fig. 8. Average BER versus PAR at different T_f.

set as 0.3. Therefore, the proposed OSS-NOMA VLC system can definitely yield a sum data rate of 800 kbps for two users with the average BER meeting the FEC threshold of 3.8×10^{-3}.

To further confirm the superiority of OSS-NOMA, we directly compare it to time division multiple address (TDMA), one of the conventional multiple access schemes. We follow the same experiment settings as above, but fix the PAR as 0.3 for OSS-NOMA, and use pulse amplitude modulation (PAM4) for user1 and user2 in TDMA to achieve the same data rate as that delivered by OSS-NOMA. Obviously, the proposed OSS-NOMA significantly outperforms the TDMA in terms of average BER, as shown in Fig. 9, because the OSS-NOMA scheme considers the user's fairness and channel difference while the TDMA ignores that. More specifically, in OSS-NOMA, the far user naturally is allocated with a higher power so as to get a reasonable BER, but the users in conventional TDMA are allocated with the same power, so the near user1 can achieve the best performance in all tests at the cost of sacrificing the far use of user2. Therefore, the proposed OSS-NOMA scheme is clearly superior to the baseline of TDMA, and all results strongly

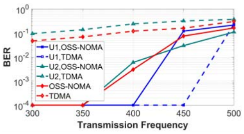

Fig. 9. Performance comparison between the proposed OSS-NOMA and conventional TDMA.

confirm the feasibility of OSS-NOMA for VLC-enabled IoT applications.

In this Letter, a novel OSS-NOMA scheme has been proposed and implemented; it pushes the advanced NOMA technique into practical VLC systems. Through theoretical analysis and field experiments, we have verified the feasibility of the proposed OSS-NOMA scheme in COTS-device-enabled VLC. In particular, by leveraging the OSS technique, only digital control is required in OSS-NOMA VLC so as to avoid the negative affect of LED nonlinearity and complicated analog circuitry. Extensive evaluations have shown the implemented OSS-NOMA VLC prototype can deliver low average BERs of $\leq 3.1 \times 10^{-3}$ for two users at a data rate of 800 kbps, which strongly confirms its promising future for VLC-enabled IoT applications.

Funding. National Natural Science Foundation of China (61902267, 61901065, 6160224); Fundamental Research Funds for the Central Universities (YJ201868, 2020CDJGFWDZ014).

Disclosures. The authors declare no conflicts of interest.

[†]These authors contributed equally to this work.

REFERENCES

1. I. Demirkol, D. Camps-Mur, J. Paradells, M. Combalia, W. Popoola, and H. Haas, IEEE Commun. Mag. **57**(6), 107 (2019).
2. S. Shao, A. Khreishah, and I. Khalil, IEEE Trans. Mobile Comput. **19**, 836 (2020).
3. A. Yang, Y. Wu, M. Kavehrad, and G. Ni, IEEE Wireless Commun. **22**, 24 (2015).
4. B. Lin, X. Tang, and Z. Ghassemlooy, IEEE Wireless Commun. Lett. **8**, 1260 (2019).
5. C. Chen, W. Zhong, H. Yang, P. Du, and Y. Yang, IEEE Wireless Commun. Lett. **8**, 568 (2019).
6. Y. Yang, C. Chen, W. Zhang, X. Deng, P. Du, H. Yang, W.-D. Zhong, and L. Chen, Opt. Express **26**, 34031 (2018).
7. Z. Yang, W. Xu, and Y. Li, IEEE Wireless Commun. Lett. **6**, 66 (2017).
8. X. Guan, Q. Yang, and C. Chan, IEEE Photon. Technol. Lett. **29**, 377 (2017).
9. C. Chen, W. Zhong, H. Yang, and P. Du, IEEE Photon. Technol. Lett. **30**, 307 (2018).
10. T. Fath, C. Heller, and H. Haas, J. Lightwave Technol. **31**, 1734 (2013).
11. A. D. Griffiths, M. S. Islim, J. Herrnsdorf, J. J. D. McKendry, R. Henderson, H. Haas, E. Gu, and M. D. Dawson, Opt. Express **25**, A338 (2017).
12. M. S. A. Mossaad, S. Hranilovic, and L. Lampe, IEEE Trans. Commun. **63**, 4304 (2015).
13. T. Komine and M. Nakagawa, IEEE Trans. Consum. Electron. **50**, 100 (2004).